This is the accepted manuscript made available via CHORUS. The article has been published as:

# Interplay of symmetry breaking and deconfinement in three-dimensional quantum vertex models

Shankar Balasubramanian, Daniel Bulmash, Victor Galitski, and Ashvin Vishwanath

Phys. Rev. B **110**, L180401 — Published 6 November 2024

DOI: 10.1103/PhysRevB.110.L180401

# Interplay of symmetry breaking and deconfinement in 3D quantum vertex models

Shankar Balasubramanian,[1] Daniel Bulmash,[2] Victor Galitski,[3] and Ashvin Vishwanath[4]

[1] *Center for Theoretical Physics, Massachusetts Institute of Technology, Cambridge, MA 02139, USA*
[2] *Joint Quantum Institute and Condensed Matter Theory Center, Department of Physics, University of Maryland, College Park, Maryland 20742-4111, USA*
[3] *Department of Physics, University of Maryland, College Park, Maryland 20742-4111, USA*
[4] *Department of Physics, Harvard University, Cambridge, MA 02138, USA*

We construct a broad class of frustration-free *quantum vertex models* in 3+1D whose ground states are weighted superpositions of classical 3D vertex model configurations. Our results are illustrated for diamond, cubic, and BCC lattices, but hold in general for 3D lattices with even coordination number. The corresponding classical vertex models have a $\mathbb{Z}_2$ gauge constraint enriched with a $\mathbb{Z}_2$ global symmetry. We study the interplay between these symmetries by exploiting exact wavefunction dualities and effective field theories. We find an exact gapless point which by duality is related to the Rokhsar-Kivelson (RK) point of $U(1)$ spin liquids. At this point, both the symmetry breaking and deconfinement order parameters exhibit long range order. The gapless point is additionally a self-dual point of a second duality that maps the $\mathbb{Z}_2$ deconfined and $\mathbb{Z}_2$ symmetry-broken phases to one another. For the BCC lattice vertex model, we find that gapless point is proximate to an unusual intermediate phase where symmetry breaking and deconfinement coexist.

*Introduction*— Quantum spin liquids represent zero temperature phases of matter whose essential characteristics lie beyond the Landau order parameter paradigm [1]. Quantum dimer models represent a family of simplified models [2–6] where novel properties of quantum spin liquids such as fractionalized excitations, emergent gauge bosons and ground state degeneracy can be readily accessed. Analytic progress is aided by the fact that at specially tuned Rokhsar-Kivelson (RK) points [3], correlation functions in the ground state of quantum dimer models match correlation functions in classical dimer models [3, 7–10], which can be exactly computed in two dimensions [11, 12]. Due to the dearth of exactly solvable statistical mechanics models in three dimensions, less is understood about the general phase structure of 3+1D quantum dimer models, although exotic phases such as $U(1)$ spin liquids are known to exist [13–15].

In this paper, we study a family of 3+1D quantum dimer models enriched with a global $\mathbb{Z}_2$ dimer flip symmetry. At suitably defined RK points, these models have ground states that are weighted superpositions of configurations in a 3D classical vertex model, a statistical mechanics model of interacting loops. We call these *quantum vertex models*; prior work on such models has focused on the 2D square lattice [16, 17], with recent work generalizing to other 2D lattices [18]. The 3+1D quantum vertex models exhibit a quantum phase transition between a deconfined phase and a phase which spontaneously breaks the $\mathbb{Z}_2$ symmetry – this transition can be mapped to a thermodynamic phase transition in the 3D classical vertex models. The exact location of the transition point can be determined with the help of *two* different dimension-independent self dualities found in classical vertex models. In 3+1D, the gapless transition point has the unusual property that local dimer order and deconfinement coexist. We also construct a quantum vertex model where the gapless point is proximate to a phase where dimer and deconfinement order parameters acquire nonzero expectation values. This proximate phase bears resemblance to fragmented Coulomb phases [19–23] but is found in a qualitatively different setting. We use effective field theory methods to study the phase structure near this multicritical point and to analyze deformations of the quantum vertex model away from the RK manifold.

*Quantum vertex models*— We construct a Hamiltonian defined on a regular bipartite lattice in 3D with even coordination number. We will focus on three cases, where the bipartite lattice is (i) a diamond lattice, dual to the pyrochlore lattice of corner sharing tetrahedra, (ii) a cubic lattice, dual to a lattice of corner sharing octahedra, and (iii) a BCC lattice, dual to a lattice of corner sharing cubes. However, our results generically hold for *any* even-coordinated lattice in 3D.

We start by briefly defining a classical vertex model, whose degrees of freedom are dimers on the links of the lattice. The classical Boltzmann weight $\mathcal{W}(C)$ of a configuration $C$ of dimers is the product of vertex weights $W_{V_p}(n_C)$ at each site $p$, where $n_C$ is the number of dimers touching $p$ in configuration $C$ and $V_p$ is the coordination number: $\mathcal{W}(C) = \prod_p W_{V_p}(n_C)$. The partition function is then $\mathcal{Z} = \sum_C \mathcal{W}(C)$. Motivated by this construction, we define an (unnormalized) RK ground state wavefunction $|\mathrm{GS}\rangle = \sum_C \sqrt{\mathcal{W}(C)}\,|C\rangle$, whose norm is the partition function of the classical vertex model.

We now discuss the choice of vertex weights. We explicitly impose a $\mathbb{Z}_2$ symmetry of exchanging dimers and empty links in the vertex weights: for the 8-vertex model on a diamond lattice

$$W_4(0) = W_4(4) = u, \qquad W_4(2) = 1, \tag{1}$$

for the 32-vertex model on a cubic lattice

$$W_6(0) = W_6(6) = u, \qquad W_6(2) = W_6(4) = 1, \tag{2}$$

and for the 128-vertex model on the BCC lattice

$$W_8(0) = W_8(8) = u, \quad W_8(2) = W_8(6) = v, \quad W_8(4) = 1. \tag{3}$$

For the diamond and BCC lattices, $u = v = 0$ corresponds to an ice rule constraint where the number of dimers equals the number of empty links at each site. On the cubic lattice, the ice rule constraint requires three dimers per site [15]. These points have an emergent $U(1)$ gauge structure, and in the diamond and cubic lattices correspond to RK points of known $U(1)$ spin liquid phases [14, 15]. Using an exact duality, we show that these points are mapped to $u = 3$ on the diamond lattice, $u = 5$ on the cubic lattice, and $u = 35/3, v = 5/3$ on the BCC lattice. These gapless points will be a large focus of this paper.

We may also construct a frustration-free Hamiltonian whose ground state is the RK wavefunction $|\mathrm{GS}\rangle = \sum_C \sqrt{\mathcal{W}(C)}\,|C\rangle$, and therefore shares the same RK phase diagram as the classical vertex model. This construction is standard and covered in the Supplementary Material (see [24] and Refs. [18, 25, 26] therein). Define an operator $P$ that projects onto an even dimer constraint at each site. Schematically, the Hamiltonian may be written as $H = P + H_A + rH_B$, where

$$H_A = \sum_{C_\ell,\ell} \frac{1}{\omega_{u,v}(C_\ell)} \left|C_\ell\rangle\langle C_\ell\right| + \omega_{u,v}(C_\ell) \left|\overline{C}_\ell\rangle\langle \overline{C}_\ell\right| \tag{4}$$

$$H_B = -\sum_{C_\ell,\ell} \left|C_\ell\rangle\langle \overline{C}_\ell\right| + \left|\overline{C}_\ell\rangle\langle C_\ell\right| \tag{5}$$

with $\omega_{u,v}$ a certain scalar function of $u$ and $v$, $\ell$ corresponding to a minimal length loop on the lattice (squares on the cubic and BCC lattices, and hexagons in the diamond lattice), $C_\ell$ a configuration of spins on $\ell$, and $\overline{C}_\ell$ the opposite configuration of spins. The RK wavefunction is a ground state for $r = 1$. As in the classical vertex model, this Hamiltonian has a global $\mathbb{Z}_2$ spin-flip symmetry $\prod_i X_i$ interchanging dimers and empty links.

*Dualities and phase diagrams*— Classical statistical mechanics in 3D is known to admit very few exact solutions [27–29]; however, conveniently, vertex models possess a self-duality which is a special case of Wegner's duality [18, 30–32] and holds in all dimensions. This duality exactly relates the partition functions of classical vertex models for vertex weights $(u, v)$ and $(u^*, v^*)$. One can show that for an 8-vertex model on a diamond lattice, Wegner's duality gives $u^* = (3 + u)/(u - 1)$, which indicates that $u = 3$ is a self dual point [33–36]. For the 32-vertex model on a cubic lattice, Wegner's duality gives $u^* = (15 + u)/(u - 1)$, so that $u = 5$ is the self dual point. These coincide with the gapless points previously discussed. For the BCC lattice, Wegner's duality gives $u^* = (35 + u + 28v)/(3 + u - 4v)$ and $v^* = (-5 + u + 4v)/(3 + u - 4v)$, yielding the self-dual line $u - 4v = 5$ which contains the gapless point $u = 35/3, v = 5/3$.

On the diamond and BCC lattices, there is a second self-duality, which we call the decorated Wegner duality. It can be shown that the partition function formally obeys $\mathcal{Z}(u) = \mathcal{Z}(-u)$ on the diamond lattice and $\mathcal{Z}(u, v) = \mathcal{Z}(u, -v)$ on the BCC lattice. Composing this identity with Wegner's duality gives $\mathcal{Z}(\mathsf{u}^*, \mathsf{v}^*) = \mathcal{Z}(u, v)$ where $\mathsf{u}^* = (3 - u)/(u + 1)$ for the diamond lattice, and $\mathsf{u}^* = (35 + u - 28v)/(3 + u + 4v)$ and $\mathsf{v}^* = (5 - u + 4v)/(3 + u + 4v)$ for the BCC lattice. For these lattices, this duality maps the ice rule point $u = v = 0$ to the gapless point.

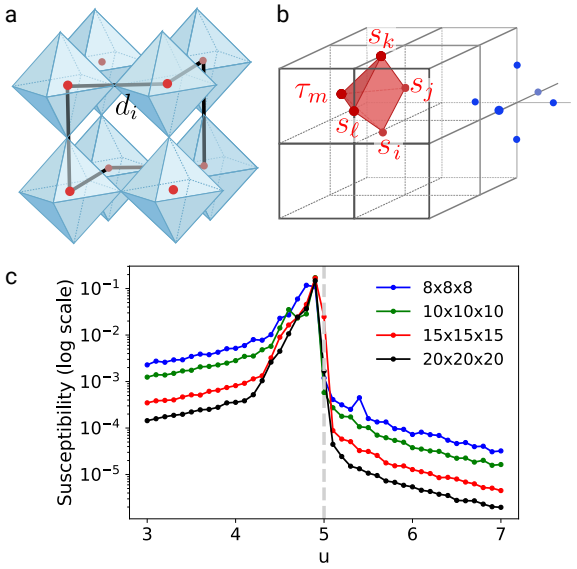



FIG. 1. The dual lattice of the octahedral lattice is a cubic lattice, where the vertex model is defined (a). The spin model derived in the Appendix is shown in (b), with gauge symmetries indicated by the blue dots and the 5-spin interaction indicated by the red pyramids. Monte Carlo simulations of the dimer susceptibility suggest a transition at $u = 5$.

The quantum vertex models feature additional special points. At the point $u = v = 1$, the parent Hamiltonian becomes the 3D toric code on the respective dual lattice [37], and thus the phase diagram must include a gapped phase with $\mathbb{Z}_2$ topological order. At $u = \infty$, one finds a phase that breaks the global $\mathbb{Z}_2$ symmetry. The gapless point indicates a phase transition between the deconfined and symmetry broken phases; for all three lattices we performed Monte Carlo simulations to verify this (see Figures 1[c], 2[d], and 3). Other ground state transitions out of the toric code phase were numerically studied in Refs. [38–40] and thermal transitions were studied in Refs. [41, 42].

*Effective field theories*— We now proceed to characterizing the gapless points ($u = 5$ for cubic, $u = 3$ for diamond, and $(u, v) = (35/3, 5/3)$ for BCC) by deriving an effective field theory. To do so, we observe that it is possible to introduce a new formulation of the vertex model in terms of height variables via the following exact

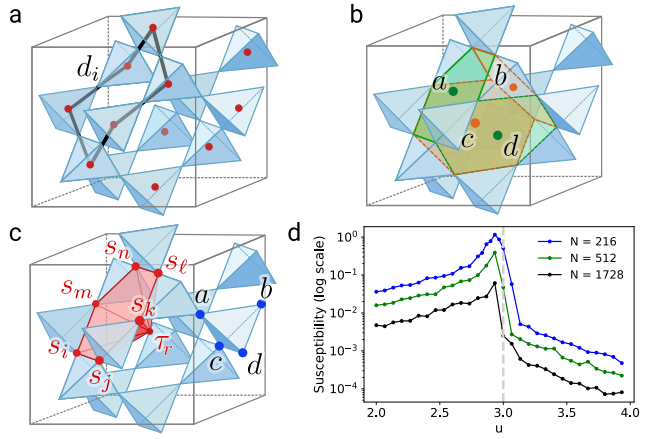



FIG. 2. The pyrochlore lattice is shown in (a), with dimers on the diamond lattice labelled. Panels (b) and (c) are relevant for the mapping to a classical spin model, which is derived in the Appendix. The spins $s_i$ are placed on the centers of the hexagons (b) forming a dual pyrochlore lattice shown in (c). On the dual pyrochlore lattice, the gauge symmetry is on the tetrahedra and the 7-spin interaction is labelled. Monte Carlo simulations of the dimer susceptibility show a phase transition around $u = 3$ in (d) and $N$ denotes the number of sites in the simulation.

rewriting of the partition function at the self dual point:

$$\mathcal{Z}_0 = \int_0^{2\pi} d^n\theta \prod_{\langle p,q\rangle} \cos\left(\theta_p - \theta_q\right), \tag{6}$$

where $p$ and $q$ are sites on the diamond, cubic, or BCC lattices. Interpreting $\theta_p$ as height fields, in the long wavelength limit, we assume that fluctuations of this field are small and can postulate a Euclidean field theory

$$\mathcal{Z}_0 = \int \mathcal{D}\theta(x)\, \exp\left(-\frac{K}{2}\int d^3x\, (\nabla\theta)^2 + \cdots\right), \tag{7}$$

which has an global $U(1)$ symmetry due to the shift invariance of $\theta$. A different height field representation was previously proposed for the 2D 8-vertex model on a square lattice [43, 44]. To understand this emergent $U(1)$ symmetry, recall that the decorated Wegner duality maps an ice rule constrained model to the gapless point. In the ice rule limit, one can construct a vector potential and formulate an effective action equivalent to $U(1)$ gauge theory in $2+1$D [13]. This action has a hidden $U(1)_{\text{top}}$ symmetry corresponding to the monopole charge (where the operator that creates a monopole in the $U(1)$ gauge theory is $\mathcal{M}_{\boldsymbol{x}} = e^{i\theta(\boldsymbol{x})}$). The decorated Wegner duality thus maps a $U(1)$ gauge theory in $2+1$D to a "dual photon", where the $U(1)_{\text{top}}$ symmetry is manifested as a global shift symmetry; this duality both extends over a large parameter regime and is exact on the lattice. Electric field correlations are equivalent to dimer correlations, which are dipolar in the ice rule limit: $\langle s_i(\boldsymbol{x}) s_j(\boldsymbol{y})\rangle \sim \frac{1}{r^5}(3r_i r_j - r^2\delta_{ij})$, where $\boldsymbol{r} = \boldsymbol{y} - \boldsymbol{x}$. This is consistent with the effective field theory as under the decorated Wegner duality, the correlation function maps to $\langle s_i(\boldsymbol{x}) s_j(\boldsymbol{y})\rangle = \langle \tan\left(\theta_{\boldsymbol{x}} - \theta_{\boldsymbol{x}+\boldsymbol{e_i}}\right) \tan\left(\theta_{\boldsymbol{y}} - \theta_{\boldsymbol{y}+\boldsymbol{e_j}}\right)\rangle \approx \langle \partial_i\theta(\boldsymbol{x})\partial_j\theta(\boldsymbol{y})\rangle$, which also has a dipolar form.

Next, we compute the spontaneous dimer density near the gapless point, $\langle d_i(\boldsymbol{x}) d_j(\boldsymbol{y})\rangle$, which can be shown to be $\left\langle \frac{\cos\left(\theta_{\boldsymbol{x}}+\theta_{\boldsymbol{x}+\boldsymbol{e_i}}\right)}{\cos\left(\theta_{\boldsymbol{x}}-\theta_{\boldsymbol{x}+\boldsymbol{e_i}}\right)} \frac{\cos\left(\theta_{\boldsymbol{y}}+\theta_{\boldsymbol{y}+\boldsymbol{e_i}}\right)}{\cos\left(\theta_{\boldsymbol{y}}-\theta_{\boldsymbol{y}+\boldsymbol{e_i}}\right)} \right\rangle$ and maps onto $\langle \cos(2\theta(\boldsymbol{x}))\cos(2\theta(\boldsymbol{y}))\rangle$ in the long-wavelength limit. For a compact boson in three dimensions, this operator exhibits long range order. We may also consider the operator $\langle \sin(2\theta(\boldsymbol{x}))\sin(2\theta(\boldsymbol{y}))\rangle$, which on the lattice corresponds to applying two test charges at $\boldsymbol{x}$ and $\boldsymbol{y}$ and computing the ratio of partition functions with and without the charges, thus serving as a diagnostic for deconfinement (see Supplemental Material [24]). This operator also exhibits long range order, so at the gapless point local order and deconfinement coexist.

Next, we discuss what occurs when one perturbs about the gapless point, but still within $(u, v)$ space. We utilize the following exact rewriting of the partition function

$$\mathcal{Z}_\alpha = \int_0^{2\pi} d^n\theta \prod_{\langle p,q\rangle} \left(f(\theta_p) f(\theta_q) + g(\theta_p) g(\theta_q)\right), \tag{8}$$

where $f(\theta) = \cos\theta + \alpha\cos(3\theta) + \beta\cos(7\theta)$ and $g(\theta) = \sin\theta - \alpha\sin(3\theta) - \beta\sin(7\theta)$. An explicit relation between $(u, v)$ and $(\alpha, \beta)$ is presented in the Supplemental Material [24]. For the diamond and cubic lattices, $\beta = 0$, and is only nonzero for the BCC lattice. Conveniently, under Wegner's duality, $(\alpha, \beta) \to (-\alpha, \beta)$, which as an operation on the fields is equivalent to $\theta \to \theta + \pi/4$. Setting $\beta = 0$ for simplicity, and using the explicit forms for $f$ and $g$, the partition function becomes a sine-Gordon model in the long wavelength limit, to leading order in $\alpha$:

$$\mathcal{Z}_\alpha = \int \mathcal{D}\theta(x)\, \exp\left(-\frac{K}{2}\int d^3x\, (\nabla\theta)^2 - \frac{4\alpha}{K}\cos(4\theta) + \cdots\right) \tag{9}$$

At $\alpha = 0$ the $U(1)$ symmetry implies that all symmetry breaking cosine terms vanish. The $U(1)$ symmetry breaking terms are relevant, consistent with the gapless point indicating a transition. For small positive $\alpha$, $|\langle\cos(2\theta)\rangle|$ is pinned to 1, indicating a $\mathbb{Z}_2$ broken phase, and for small negative $\alpha$, $\langle\cos(2\theta)\rangle$ is pinned to 0, indicating a $\mathbb{Z}_2$ unbroken phase. The deconfinement operator $|\langle\sin(2\theta)\rangle|$ is 0 when $\alpha$ is positive and 1 when $\alpha$ is negative, consistent with it being a diagnostic of topological order. Under Wegner's duality, $\cos(2\theta)$ and $\sin(2\theta)$ are exchanged at the gapless point.

For nonzero $\beta$ on the BCC lattice, the effective action becomes

$$\mathcal{S}[\alpha,\beta] = \frac{K}{2}\int d^3x\, (\nabla\theta)^2 - \frac{4\alpha}{K}\cos(4\theta) - \frac{4\beta}{K}\cos(8\theta) + \cdots \tag{10}$$

consistent with $\beta$ coupling to a duality-even operator. Since $\cos(4\theta)$ and $\cos(8\theta)$ are both relevant, we naively

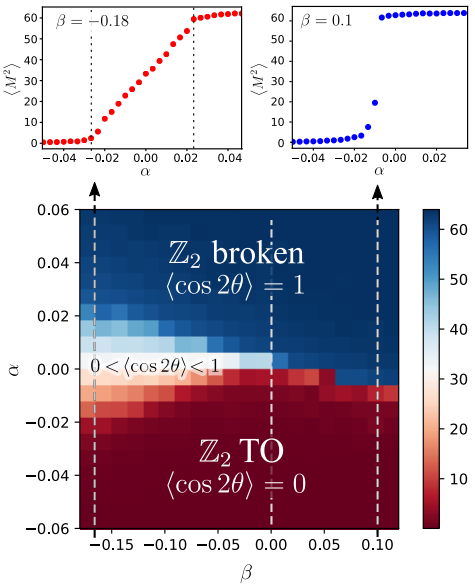



FIG. 3. Monte Carlo results for average value of the squared magnetization of an $L \times L \times L$ BCC lattice vertex model. The bottom panel ($L = 8$) this presents evidence of the existence of the intermediate phase, proximate to the gapless point at $(\alpha, \beta) = (0, 0)$. Vertical cuts are shown in the two top panels (simulations here are for $L = 12$) – in the left plot, two sharp transitions are seen and the duality maps these transition points to one another, while in the right plot, a single sharp transition occurs.

mean field theory to the effective potential $V(\theta) = \alpha \cos(4\theta) + \beta \cos(8\theta)$, which yields a first order line $\alpha = 0, \beta > 0$ between a $\mathbb{Z}_2$ broken and deconfined phase, and two second order lines in the 3D Ising universality class $\alpha \propto \pm\beta$ for $\beta < 0$. The region between these critical lines is a phase where both the dimer order parameter and the deconfinement parameter have nonzero and continuously varying expectation values; evidence for this exotic coexistence phase is seen in Monte Carlo simulations of the dimer density in the $(\alpha, \beta)$ plane, see Fig. 3.

On general grounds, one could phenomenologically arrive at the effective field theory by writing down terms consistent with invariance under the $\mathbb{Z}_2$ symmetry $\cos(2\theta) \to -\cos(2\theta)$:

$$\mathcal{S} = \int d^3x \left( \frac{K}{2} (\nabla\theta)^2 + \cdots + \sum_n c_n \cos(4n\theta) \right). \quad (11)$$

Since the local dimer density at each vertex is bounded between $-V_p$ and $+V_p$ and the operator $\cos(4n\theta)$ corresponds to changing the relative weight of vertex configurations with $k$ and $k \pm 4n$ dimers at a fixed site, we require $4n \leq V_p$, consistent with the proposed action for $V_p = 4, 6, 8$. The fact that $\cos(4n\theta)$ is duality even for $n \in 8\mathbb{Z}$ and duality odd for $n \in 8\mathbb{Z} + 4$ remains true on the lattice. Analogously to the BCC lattice, we anticipate the possibility of more interesting coexistence phases for vertex models where $V_p > 8$.

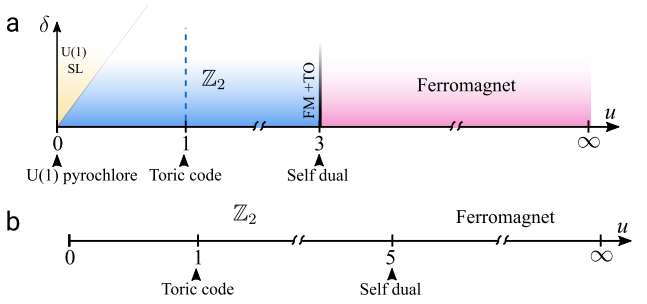



FIG. 4. Panel (a) $u$-axis (where $u$ is the vertex weight) and panel (b) show the phase diagram of the frustration free models on the diamond and cubic lattices respectively. The $\delta$-axis in panel (a) corresponds to perturbing the diamond lattice model away from the RK manifold.

Finally, we discuss the effective field theory description away from the RK manifold. Consider extending the microscopic Hamiltonian in Eqns. 4 and 5 beyond the RK point, via some generic isotropic perturbation of strength $\delta$ (as an example, we may call $\delta \sim r - 1$). As the effective field theory describing the RK wavefunction at the gapless point is a free boson, the effective field theory description for the *Hamiltonian* is a quantum Lifshitz model [2, 16, 45–47], with the imaginary time action

$$\mathcal{S} = \int d^3x\, d\tau \left( \frac{1}{2} (\partial_\tau \theta)^2 + \frac{\kappa}{2} (\nabla^2\theta)^2 + \delta (\nabla\theta)^2 \right) + \mathcal{S}_{\text{mon}}, \quad (12)$$

where $\mathcal{S}_{\text{mon}}$ accounts for monopole events: $\mathcal{S}_{\text{mon}} = \int d^3x\, d\tau \, (g_4 \cos(4\theta) + g_8 \cos(8\theta))$ [2] (we expect $g_4$ and $g_8$ to play the roles of $\alpha$ and $\beta$). The RK manifold corresponds to $\delta = 0$, and the $(\nabla^2\theta)^2$ term becomes irrelevant at $\delta > 0$, resulting in a gapless line with dynamical critical exponent $z_{\text{dyn}} = 1$ between the $\mathbb{Z}_2$ deconfined and $\mathbb{Z}_2$ broken phases. On the pyrochlore and BCC lattices the spin ice point $u = v = 0$ is expected to broaden into a $U(1)$ spin liquid phase away from the RK manifold and will always be separated from the $\mathbb{Z}_2$ broken phase by a $\mathbb{Z}_2$ deconfined phase. This follows because for the choice $\delta \sim r - 1$ the Hamiltonian at $u = 1$ always exhibits toric code topological order regardless of the value of $r$.

Furthermore, as we move along the $z_{\text{dyn}} = 1$ line (where $g_4 = g_8 = 0$), the equal-time correlators $\langle \cos(2\theta(\boldsymbol{x})) \cos(2\theta(\boldsymbol{y})) \rangle$ and $\langle \sin(2\theta(\boldsymbol{x})) \sin(2\theta(\boldsymbol{y})) \rangle$ exhibit long range order, indicating that coexistence still occurs. Studying the phase structure for $\delta > 0$ when the monopole terms are turned on, especially the stability of the coexistence phase on the BCC lattice, warrants further analytical and numerical investigations.

*Acknowledgements* – A.V. and V. G. were supported by the Simons Collaboration on Ultra Quantum Matter, a grant from the Simons Foundation (651440, A.V.). S.B. was supported by the National Science Foundation Graduate Research Fellowship under Grant No. 1745302. V.G. was also supported by NSF DMR-2037158 and US-ARO Contract No.W911NF1310172. D.B. was sup-

ported by JQI-PFC-UMD.

*Appendix on equivalent spin models*— In this Appendix we provide a different perspective on the phase structure of the 3D classical vertex models by a mapping to a classical spin model. We first illustrate this mapping for the cubic lattice vertex model, where the vertex weights are $W_6(0) = W_6(6) = u$ and $W_6(2) = W_6(4) = 1$. We first construct a dual cubic lattice, whose sites are located in the cube centers of the direct lattice. Dimers on the direct lattice therefore pierce faces of the dual lattice. We place new spins on the edges of this dual lattice so that each dimer on the direct lattice is surrounded by four spins $s_1, \cdots, s_4$ on the dual lattice. The dimer variable is mapped to spins as $d = s_1 s_2 s_3 s_4$; this automatically respects the even dimer constraint due to $\prod_{\square \in \square} s_i s_j s_k s_\ell = \prod_{-\in \square} s_i^2 = 1$. The Boltzmann weight enforcing the even dimer constraint at a given vertex with vertex weights $W_6(n)$ is therefore

$$W_{\square}(\vec{s}) = \cosh\left(\mathcal{J} \sum_{\square \in \square} s_i s_j s_k s_\ell\right), \tag{13}$$

where $\frac{\cosh 6\mathcal{J}}{\cosh 2\mathcal{J}} = u$. The full partition function is therefore

$$\mathcal{Z}_{\text{spin}} = \sum_{\vec{s}} \prod_{\square} W_{\square}(\vec{s}) = \sum_{\vec{s},\vec{\tau}} \exp\left(\mathcal{J} \sum_{p} s_i s_j s_k s_\ell \tau_m\right), \tag{14}$$

where in the second equality we converted the cosh to an exponential by adding a new 'ghost' spin $\tau$ at the center of each cube on the dual lattice; the subscript $p$ denotes a pyramid formed from four spins identifying a dimer and a ghost spin (see Figure 1[b]).

First, the standard $\mathbb{Z}_2$ gauge symmetry $P = \prod_{i \in v} X_i = X_1 X_2 X_3 X_4 X_5 X_6$ is easily seen, where $X_i$ is the spin flip operator acting on $s_i$, and $i \in v$ denotes spins $s_i$ on the edges connected to site $v$, see Fig. 1[b] (shown as blue dots). Moreover, the gauge theory is enriched with a global $\mathbb{Z}_2$ symmetry corresponding to the operator mapping $d_i \to -d_i$ and $\tau_i \to -\tau_i$ (the global transformation $d_i \to -d_i$ requires flipping some subset of the $s$ spins, see Supplementary Material [24]). As a result, an unusual aspect of this gauge theory is that the scaling of the Wilson loop $W_C = \langle \prod_{i \in C} s_i \rangle$ exhibits what we call an 'even-odd' behavior. At large $\mathcal{J}$ the Wilson loops obey a perimeter law behavior, a consequence of simultaneous deconfinement and breaking of the global $\mathbb{Z}_2$ symmetry. When $\mathcal{J}$ is small, Wilson loops enclosing an *even* number of plaquettes obeys an area law, while Wilson loops enclosing an *odd* number of plaquettes are zero. This follows because odd Wilson loops are charged under the global symmetry while even Wilson loops are not.

On the diamond lattice, one can construct an analogous spin model. The dimers live on the sites of a pyrochlore lattice, and we assign a spin $s_i$ to the center of each hexagon of the pyrochlore lattice. The spins form a dual pyrochlore lattice as illustrated in Figure 2[b], with dimers on the direct lattice piercing hexagons on the dual lattice. The dimer variables are $d_i = \prod_{j \in \widetilde{\bigcirc}_i} s_j$ where $\widetilde{\bigcirc}_i$ denotes the hexagon on the dual lattice pierced by dimer $i$ on the direct lattice. A gauge transformation corresponds to flipping the 4 spins on tetrahedra of the dual pyrochlore lattice via $P = \prod_{i \in \widetilde{\triangle}} X_i$.

We introduce a ghost spin $\tau$ at the locations indicated in Fig. 1[c], so that the partition function is

$$\mathcal{Z}_{\text{spin}} = \sum_{\vec{s},\vec{\tau}} \exp\left(\mathcal{J} \sum_{p} s_i s_j s_k s_\ell s_m s_n \tau_r\right), \tag{15}$$

with the 7-spin interaction on pyramid $p$ labelled in Figure 2[c] and $\cosh 4\mathcal{J} = u$. The Wilson loops of this classical gauge theory also exhibit an even-odd effect.

On the BCC lattice, two different effective spin models are provided in the Supplementary Material [24]: along with a global $\mathbb{Z}_2$ symmetry, one of the models has a $\mathbb{Z}_2$ gauge structure, while the other model curiously has a subsystem symmetry. The coexistence phase in the BCC lattice vertex model will also correspond to a coexistence phase in these spin models.

In the original quantum vertex model, an odd Wilson loop enclosing a single plaquette corresponds to a dimer variable, which probes the $\mathbb{Z}_2$ symmetry breaking transition. An even Wilson loop of spins corresponds to a 't Hooft loop of dimers $W_{\partial S} = \langle \prod_{i \in S} d_i \rangle$, where $\partial S$ is the boundary of open surface $S$. In addition, one has a dual Wilson loop order parameter which is a product of $X_i$ around a loop of links [16]: $\widetilde{W}_C = \langle \prod_{i \in C} X_i \rangle$.


[1] X.-G. Wen, *Quantum field theory of many-body systems: from the origin of sound to an origin of light and electrons* (Oxford University Press on Demand, 2004).

[2] E. Fradkin, *Field theories of condensed matter physics* (Cambridge University Press, 2013).

[3] D. S. Rokhsar and S. A. Kivelson, Superconductivity and the quantum hard-core dimer gas, Phys. Rev. Lett. **61**, 2376 (1988).

[4] N. Read and S. Sachdev, Spin-peierls, valence-bond solid, and néel ground states of low-dimensional quantum antiferromagnets, Phys. Rev. B **42**, 4568 (1990).

[5] N. Read and B. Chakraborty, Statistics of the excitations of the resonating-valence-bond state, Phys. Rev. B **40**, 7133 (1989).

[6] P. Fazekas and P. W. Anderson, On the ground state properties of the anisotropic triangular antiferromagnet, The Philosophical Magazine: A Journal of Theoretical Experimental and Applied Physics **30**, 423 (1974), https://doi.org/10.1080/14786439808206568.

[7] R. Moessner and S. L. Sondhi, Resonating valence bond

phase in the triangular lattice quantum dimer model, Phys. Rev. Lett. **86**, 1881 (2001).
[8] P. Fendley, R. Moessner, and S. L. Sondhi, Classical dimers on the triangular lattice, Phys. Rev. B **66**, 214513 (2002).
[9] C. L. Henley, From classical to quantum dynamics at rokhsar–kivelson points, Journal of Physics: Condensed Matter **16**, S891 (2004).
[10] G. Misguich, D. Serban, and V. Pasquier, Quantum dimer model on the kagome lattice: Solvable dimer-liquid and ising gauge theory, Phys. Rev. Lett. **89**, 137202 (2002).
[11] P. W. Kasteleyn, Dimer statistics and phase transitions, Journal of Mathematical Physics **4**, 287 (1963), https://doi.org/10.1063/1.1703953.
[12] H. N. V. Temperley and M. E. Fisher, Dimer problem in statistical mechanics-an exact result, The Philosophical Magazine: A Journal of Theoretical Experimental and Applied Physics **6**, 1061 (1961).
[13] D. A. Huse, W. Krauth, R. Moessner, and S. L. Sondhi, Coulomb and liquid dimer models in three dimensions, Phys. Rev. Lett. **91**, 167004 (2003).
[14] M. Hermele, M. P. A. Fisher, and L. Balents, Pyrochlore photons: The $u(1)$ spin liquid in a $s = \frac{1}{2}$ three-dimensional frustrated magnet, Phys. Rev. B **69**, 064404 (2004).
[15] O. I. Motrunich and T. Senthil, Origin of artificial electrodynamics in three-dimensional bosonic models, Phys. Rev. B **71**, 125102 (2005).
[16] E. Ardonne, P. Fendley, and E. Fradkin, Topological order and conformal quantum critical points, Annals of Physics **310**, 493 (2004).
[17] C. Castelnovo, C. Chamon, C. Mudry, and P. Pujol, From quantum mechanics to classical statistical physics: Generalized rokhsar–kivelson hamiltonians and the "stochastic matrix form"' decomposition, Annals of Physics **318**, 316 (2005).
[18] S. Balasubramanian, V. Galitski, and A. Vishwanath, Classical vertex model dualities in a family of two-dimensional frustrated quantum antiferromagnets, Phys. Rev. B **106**, 195127 (2022).
[19] L. Savary and L. Balents, Coulombic quantum liquids in spin-1/2 pyrochlores, Phys. Rev. Lett. **108**, 037202 (2012).
[20] S. Powell, Ferromagnetic coulomb phase in classical spin ice, Phys. Rev. B **91**, 094431 (2015).
[21] M. E. Brooks-Bartlett, S. T. Banks, L. D. C. Jaubert, A. Harman-Clarke, and P. C. W. Holdsworth, Magnetic-moment fragmentation and monopole crystallization, Phys. Rev. X **4**, 011007 (2014).
[22] E. Lhotel, L. D. Jaubert, and P. C. Holdsworth, Fragmentation in frustrated magnets: A review, Journal of Low Temperature Physics **201**, 710 (2020).
[23] V. Raban, C. T. Suen, L. Berthier, and P. C. W. Holdsworth, Multiple symmetry sustaining phase transitions in spin ice, Phys. Rev. B **99**, 224425 (2019).
[24] See the supplemental material for details.
[25] M. E. Peskin, Critical point behavior of the wilson loop, Physics Letters B **94**, 161 (1980).
[26] J. B. Kogut, An introduction to lattice gauge theory and spin systems, Rev. Mod. Phys. **51**, 659 (1979).
[27] F. Y. Wu, Phase transition in a vertex model in three dimensions, Phys. Rev. Lett. **32**, 460 (1974).
[28] A. Zamolodchikov, Tetrahedra equations and integrable systems in three-dimensional space, Sov. Phys. JETP **52**, 325 (1980).
[29] V. Bazhanov and R. Baxter, New solvable lattice models in three dimensions, Journal of Statistical Physics **69**, 453 (1992).
[30] F. Wegner, A transformation including the weak-graph theorem and the duality transformation, Physica **68**, 570 (1973).
[31] X. N. Wu and F. Y. Wu, Duality properties of a general vertex model, Journal of Physics A: Mathematical and General **22**, L55 (1989).
[32] L. Runnels, Duality relation for 32-vertex model on the triangular lattice, Journal of Statistical Physics **14**, 39 (1976).
[33] B. Sutherland, Exact results for the eight-vertex model in three dimensions, Phys. Rev. Lett. **31**, 1504 (1973).
[34] B. Sutherland, Critical exponents of the eight-vertex model in any dimension, Phys. Rev. Lett. **32**, 379 (1974).
[35] C. Thibaudier and J. Villain, On the three dimensional eight-vertex model, Journal of Physics C: Solid State Physics **5**, 3429 (1972).
[36] J. Villain, The 3-dimensional eight vertex model and the proton-proton correlation functions in ice, Solid State Communications **10**, 967 (1972).
[37] A. Y. Kitaev, Fault-tolerant quantum computation by anyons, Annals of Physics **303**, 2 (2003).
[38] S. Trebst, P. Werner, M. Troyer, K. Shtengel, and C. Nayak, Breakdown of a topological phase: Quantum phase transition in a loop gas model with tension, Phys. Rev. Lett. **98**, 070602 (2007).
[39] I. S. Tupitsyn, A. Kitaev, N. V. Prokof'ev, and P. C. E. Stamp, Topological multicritical point in the phase diagram of the toric code model and three-dimensional lattice gauge higgs model, Phys. Rev. B **82**, 085114 (2010).
[40] D. A. Reiss and K. P. Schmidt, Quantum robustness and phase transitions of the 3d toric code in a field, SciPost Physics **6**, 078 (2019).
[41] C. Castelnovo and C. Chamon, Entanglement and topological entropy of the toric code at finite temperature, Phys. Rev. B **76**, 184442 (2007).
[42] C. Castelnovo and C. Chamon, Topological order in a three-dimensional toric code at finite temperature, Phys. Rev. B **78**, 155120 (2008).
[43] H. Knops and L. Den Ouden, Renormalization connection between eight-vertex operators and gaussian operators, Annals of Physics **138**, 155 (1982).
[44] H. Knops, Renormalization connection between the eight-vertex model and the gaussian model, Annals of Physics **128**, 448 (1980).
[45] C. L. Henley, Relaxation time for a dimer covering with height representation, Journal of statistical physics **89**, 483 (1997).
[46] E. Fradkin, D. A. Huse, R. Moessner, V. Oganesyan, and S. L. Sondhi, Bipartite rokhsar–kivelson points and cantor deconfinement, Phys. Rev. B **69**, 224415 (2004).
[47] A. Vishwanath, L. Balents, and T. Senthil, Quantum criticality and deconfinement in phase transitions between valence bond solids, Phys. Rev. B **69**, 224416 (2004).